




Improved triboelectric performance of polydimethylsiloxane reinforced with ferroelectric composite oxide

Bin Li¹, Hongbo Liu^{1,*}, Ying Sun¹, Yule Cao¹, and Yinben Guo^{1,*} 

¹ School of Materials Engineering, Shanghai University of Engineering Science, Shanghai 201620, China

Received: 30 October 2021

Accepted: 5 January 2022

Published online:
18 January 2022

© The Author(s), under exclusive licence to Springer Science+Business Media, LLC, part of Springer Nature 2022

ABSTRACT

Triboelectric nanogenerator (TENG) has received a great deal of recent attention because it can convert mechanical energy into electrical energy. We report the synthesis of $\text{Bi}_{0.5}\text{Na}_{0.5}\text{TiO}_3\text{-BaSnO}_3/\text{NaNbO}_3\text{-SrTiO}_3$ (BNT-BS/NN-ST) ferroelectrics and the filling of BNT-BS/NN-ST particles into polydimethylsiloxane (PDMS). The effect of this inorganic material as fillers on the electrical output performance was also studied. The aim was to obtain flexible TENGs with higher output properties. It was found that the BNT-BS/NN-ST samples were well crystallized and polycrystalline and all ceramics had dense and fine-grained structures. After combining BNT-BS and NN-ST phases together, the BNT-BS/NN-ST ferroelectrics exhibited excellent thermal stability. In particular, we found that the ferroelectric/PDMS composites possessed obviously higher output voltages as compared to the pure PDMS. The values of voltage for five samples with different weight ratios (5%, 10%, 15%, 20%, and 25%) were about 194, 268, 370, 238, and 236 V, respectively.

1 Introduction

In recent years, flexible electronic products have exhibited rapid growth [1–5]. Triboelectric nanogenerator (TENG) is an electronic device based on the triboelectric effect that can convert mechanical energy of the external environment into electrical energy [6–9]. As a sustainable power source, TENG has great application prospects in the field of energy harvesting because of its advantages of flexible structure and lightweight [10, 11].

Tribo-material is one of the most critical components in TENGs. It is an extremely important research direction to improve the electrical outputs of TENGs through the design and preparation of tribo-materials. However, with the deepening of research, the optimization effect of organic tribo-materials is becoming saturated. Although many inorganic ferroelectric tribo-materials have high dielectric constants, it is difficult for them to achieve flexibility. Therefore, the organic and inorganic composites have recently received an increasing interest for their excellent dielectric properties and coupling

Address correspondence to E-mail: bohongliu@gmail.com; guoyb@sues.edu.cn

mechanisms to enhance the electrical output performances [12–19].

Recently, $\text{Bi}_{0.5}\text{Na}_{0.5}\text{TiO}_3$ (BNT) and NaNbO_3 (NN) ferroelectrics have received considerable attention as energy storage materials [20, 21]. It has been found that the BNT– BaSnO_3 (BS) relaxor ferroelectrics exhibited the coexistence of high polarization and slim polarization–electric field loops [22]. Meanwhile, it has been reported that the NN– SrTiO_3 (ST) anti-ferroelectrics possessed high dielectric constant and excellent energy storage properties [23]. To improve the electrical performances, the BNT–BS/NN–ST composite ferroelectrics were prepared by solid-state reaction in this paper and their dielectric properties were studied. Then the ferroelectric particles were filled into polydimethylsiloxane (PDMS), and the effect of this inorganic material as fillers on the output property of TENGs was investigated.

2 Experimental

2.1 Preparation of ceramics

The 0.78BNT–0.22BS/0.82NN–0.18ST ceramics were prepared via a traditional solid-state reaction process using Bi_2O_3 , Na_2CO_3 , TiO_2 , BaCO_3 , SnO_2 , Nb_2O_5 , and SrCO_3 as starting materials. All these oxides or carbonates used in this study were of analytical grade. To synthesize the BNT–BS and NN–ST, above powders were weighed according to the stoichiometric ratios and ball-milled in ethanol for 10 h. After drying, both the BNT–BS and NN–ST mixtures were calcined at 850 °C for 5 h. Then, the BNT–BS and NN–ST powders were mixed according to different molar ratios (100/0, 75/25, 50/50, 25/75, and 0/100) and ball-milled again for 20 h. The dried BNT–BS/NN–ST mixtures were pressed into disks with 10 MPa using polyvinyl alcohol (PVA) solution as the binder. After burning out the PVA at 600 °C, the disk

samples were sintered at 1150–1350 °C for 2 h depending on their components.

2.2 Fabrication of TENGs

In order to prepare ferroelectric/PDMS composite films, the BNT–BS and NN–ST powders calcined at 850 °C were mixed according to the molar ratio of 75/25 and ball-milled for 20 h. The mixed powders were then sintered at 1050 °C for 2 h and ball-milled again for 20 h to synthesize BNT–BS/NN–ST particles. These particles were firstly dispersed into PDMS (Sylgard 184, Dow Corning) solution with different weight ratios (5%, 10%, 15%, 20%, and 25%). Then, the ferroelectric/PDMS mixtures were poured into the molds and cured at 80 °C for 2 h to obtain composite films with the same thickness. Finally, the films were cut into small pieces with a size of $2 \times 3 \text{ cm}^2$ and the thin Al foil was adhered onto one side of films to fabricate the contact separation TENGs. The formation process of a BNT–BS/NN–ST/PDMS composite film is showed in Fig. 1. We can see that both of the BNT–BS/NN–ST particles and BNT–BS/NN–ST/PDMS film exhibit white color, and the film on Al foil is flexible with a thickness of $\sim 460 \mu\text{m}$.

2.3 Characterization

The phase compositions of BNT–BS/NN–ST ceramics were carried out by X-ray diffraction (XRD) on an X'Pert PRO PANalytical diffractometer. The surface morphologies of samples were studied by scanning electron microscopy (SEM, Phenom-World BV, G2pro). The dielectric properties of ceramics coated with silver electrodes onto both sides were investigated using an impedance analyzer (Keysight E4990A). The vertical force was applied on TENGs at frequency of 2 Hz by a self-made mechanical motor and then an oscilloscope (Tektronix, TBS 1202C) was used to record the output voltages.

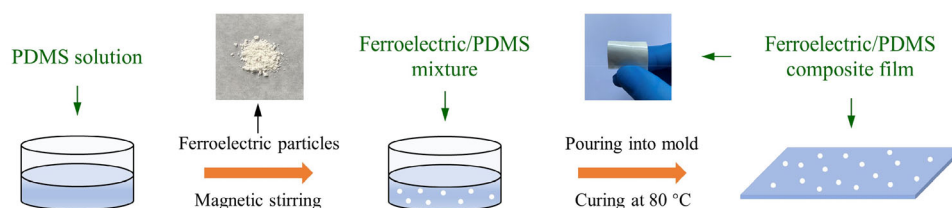


Fig. 1 Schematic diagram of the preparation process of a BNT–BS/NN–ST/PDMS composite film (left inset: photograph of the BNT–BS/NN–ST particles with a molar ratio of 75/25, right inset: photograph of the flexible BNT–BS/NN–ST/PDMS film on Al foil)

3 Results and discussion

The XRD patterns of BNT-BS/NN-ST composite samples are illustrated in Fig. 2a. Typical perovskite structure can be identified in all ceramics, and the appearance of characteristic peaks reveals that five

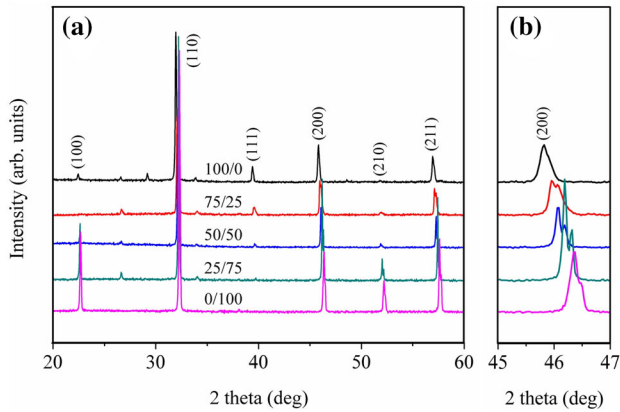


Fig. 2 a XRD patterns and b enlarged patterns around 46° of BNT-BS/NN-ST ceramics

samples are polycrystalline. It can be seen that the (111) peak intensity increases with increasing the concentration of BNT-BS. Figure 2b shows that only one (200) diffraction peak is displayed at 45°–47° for the BNT-BS relaxor ferroelectrics. And after complexing with different molar ratios of NN-ST anti-ferroelectrics, the BNT-BS/NN-ST composite ferroelectrics present splitting peaks in this range. This result confirms that three BNT-BS/NN-ST composites possess a pseudocubic phase structure. Meanwhile, the above splitting peaks shift toward larger 2θ angles with the increase of NN-ST’s content, which is attributed to the decrease in the lattice volume. This observation is similar to the previous report for NN-BNT ceramics [24].

The surface morphologies of BNT-BS/NN-ST ceramics are presented in Fig. 3a–e. It can be seen that all samples have fine grained and dense structures, which indicate that they are well crystallized. As shown in Fig. 3a and e, the average grain on the NN-ST surface is significantly larger than of the BNT-BS. The average grain sizes of NN-ST and

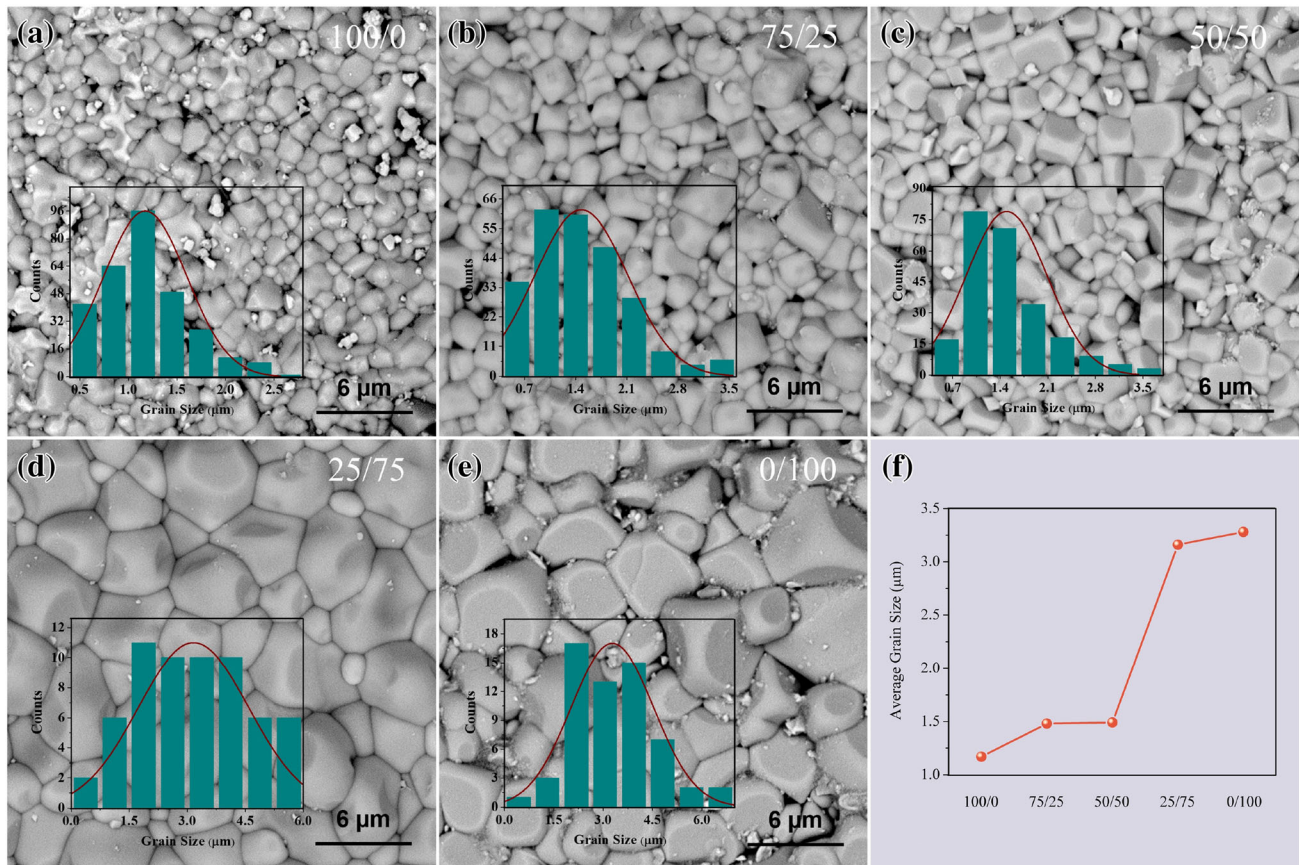


Fig. 3 a–e SEM images (insets: corresponding grain size distributions) and f average grain sizes of BNT-BS/NN-ST ceramic surfaces

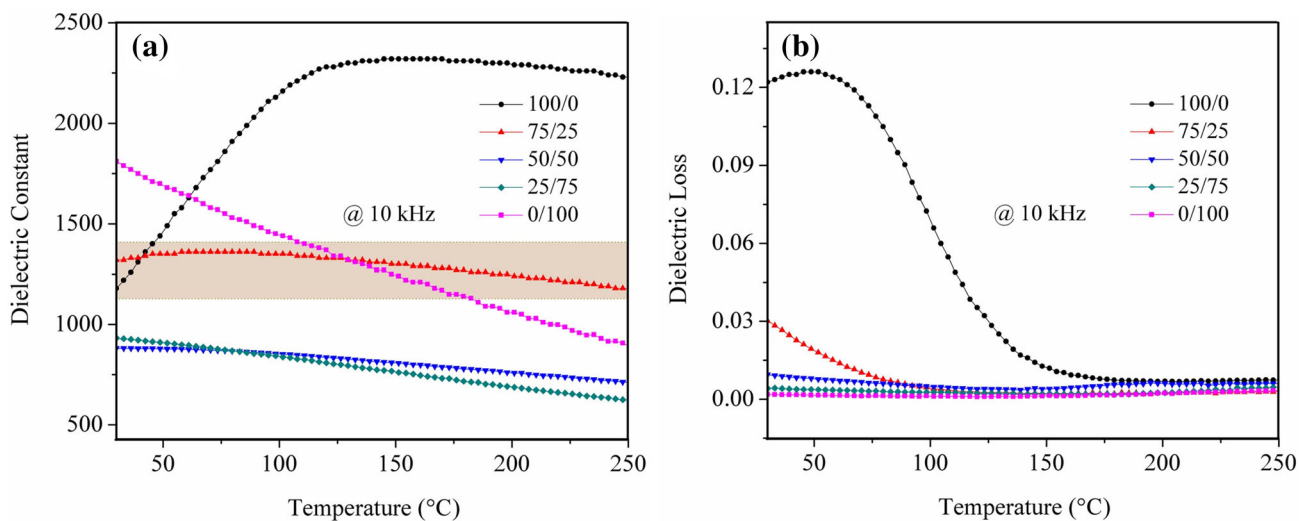


Fig. 4 Temperature dependence of **a** dielectric constant and **b** dielectric loss for BNT-BS/NN-ST ceramics

BNT-BS ceramics are about 3.28 and 1.17 μm , respectively (Fig. 3f). We can see that the average grain size of BNT-BS/NN-ST composites decreases with the increase of BNT-BS addition. Meanwhile, the fine grains are beneficial to improve dielectric breakdown strength due to the high resistivity of grain boundaries [25]. And the average grain sizes of the 25/75, 50/50, and 75/25 composites are approximately 3.16, 1.49, and 1.48 μm , respectively.

As plotted in Fig. 4, the dielectric constants and dielectric losses of BNT-BS/NN-ST ferroelectrics were investigated from room temperature to 250 °C. Compared to the BNT-BS and NN-ST ceramics, three

BNT-BS/NN-ST composites show obviously better stability against temperature (Fig. 4a). In particular, the BNT-BS/NN-ST (75/25 molar ratio) sample possesses an excellent thermal stability and a high dielectric constant value of 1320 measured at 10 kHz and room temperature. The results indicate that the 75/25 sample in this study has a large potential for temperature stable applications and a similar result has been reported for the BNT-NN ceramics [26]. In addition, it is found that three BNT-BS/NN-ST composites exhibit low dielectric losses and high temperature stability (Fig. 4b).

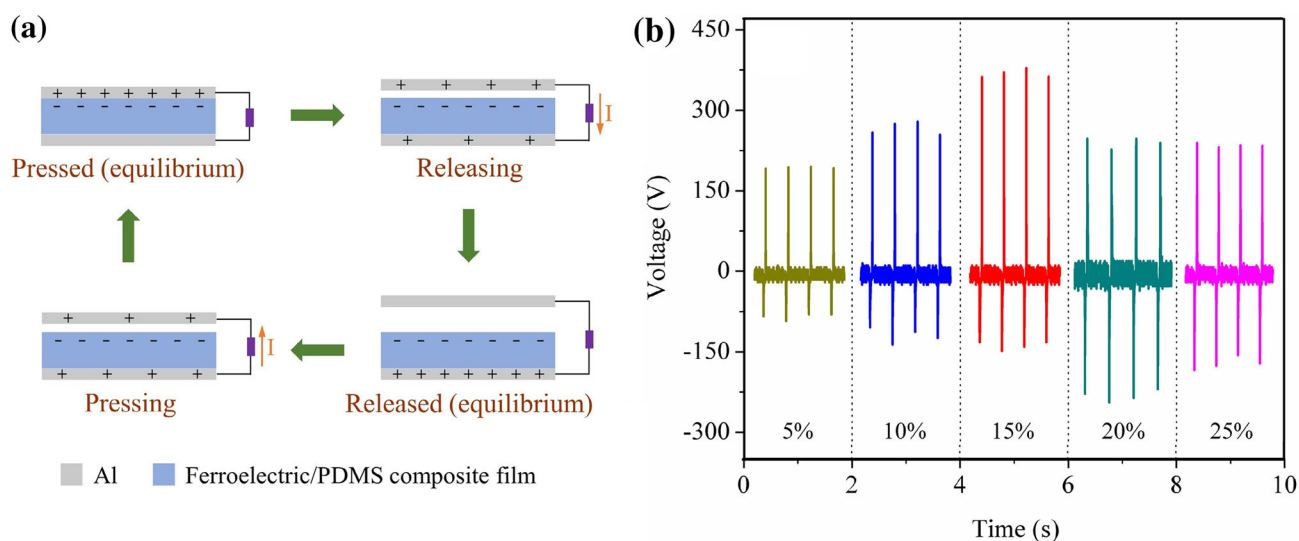


Fig. 5 **a** Schematic illustration of the working mechanism of a contact separation TENG in this study, **b** output voltages of TENGs based on composite films with different weight ratios of BNT-BS/NN-ST (75/25 molar ratio) particles

The working mechanism of a contact separation TENG is illustrated in Fig. 5a. In the pressed state, the BNT-BS/NN-ST/PDMS film acquires negative triboelectric charges. In the releasing state, the resulting charge separation will induce the current flow in external circuit. Subsequently, the opposite current signal will be generated in external circuit under the pressing state. The output voltages of TENGs based on films with five weight ratios of BNT-BS/NN-ST particles are plotted in Fig. 5b. It is found that the voltages first increase and then decrease with increasing the BNT-BS/NN-ST concentration and the voltage of TENG with weight ratio of 15% is the highest in this work. This may be due to the agglomerations of BNT-BS/NN-ST particles in films when the weight ratios are above 15%, thereby reducing their output characteristics. The voltage values of five samples (5%, 10%, 15%, 20%, and 25%) were measured approximately 194, 268, 370, 238, and 236 V, respectively. In particular, all BNT-BS/NN-ST/PDMS composites have obviously larger values as compared to the pure PDMS (~ 102 V). The results imply that using BNT-BS/NN-ST particles as fillers can significantly improve the output property of PDMS-based TENGs.

4 Conclusion

In summary, the BNT-BS/NN-ST ferroelectrics were synthesized using solid-state reaction method. The phase compositions, surface morphologies, and dielectric properties of the BNT-BS/NN-ST ceramics were detected. And the influence of the BNT-BS/NN-ST particles as fillers on the output performance of TENGs was also investigated. All ceramic samples with strong diffraction peaks were obtained after sintering 1150–1350 °C for 2 h and they had polycrystalline and fine-grained structures. It was found that three BNT-BS/NN-ST composite ceramics exhibited a pseudocubic phase structure. In addition, the BNT-BS/NN-ST composites possessed excellent thermal stability by combining relaxor ferroelectric BNT-BS and anti-ferroelectric NN-ST. Compared to the pure PDMS film, the BNT-BS/NN-ST/PDMS composite films presented significantly larger voltages and the output value of sample with weight ratio of 15% was the highest in this work. Further study on electrical performance of ferroelectric based

tribo-materials will be carried out using the first principle calculations in our next research.

Acknowledgements

This work was supported by National Natural Science Foundation of China (51903151) and Shanghai “ChenGuang” Project (19CG66).

Author contributions

BL, HL, and YG contributed to the study design, data analysis, and writing. The material preparation and data collection were performed by BL, YS, and YC.

Data availability

All data generated or analyzed during this study are included in this article.

Declarations

Conflict of interest The authors declare that they have no known competing financial interests or personal relationships that could have appeared to influence the work reported in this paper.

References

1. X.L. Shi, W.Y. Chen, T. Zhang, J. Zou, Z.G. Chen, *Energy Environ. Sci.* **14**, 729 (2021)
2. Y. Sun, T. Liu, Y. Kan, K. Gao, B. Tang, Y. Li, *Small Sci.* **1**, 2100001 (2021)
3. Z. Wang, K. Gao, Y. Kan, M. Zhang, C. Qiu, L. Zhu, Z. Zhao, X. Peng, W. Feng, Z. Qian, X. Gu, A.K.Y. Jen, B.Z. Tang, Y. Cao, Y. Zhang, F. Liu, *Nat. Commun.* **12**, 332 (2021)
4. K. Gao, Y. Kan, X. Chen, F. Liu, B. Kan, L. Nian, X. Wan, Y. Chen, X. Peng, T.P. Russell, Y. Cao, A.K.Y. Jen, *Adv. Mater.* **32**, 1906129 (2020)
5. K. Gao, J. Miao, L. Xiao, W. Deng, Y. Kan, T. Liang, C. Wang, F. Huang, J. Peng, Y. Cao, F. Liu, T.P. Russell, H. Wu, X. Peng, *Adv. Mater.* **28**, 4727 (2016)
6. Y. Cao, Y. Guo, Z. Chen, W. Yang, K. Li, X. He, J. Li, *Nano Energy* **92**, 106689 (2022)
7. S. Meti, H.P. Sagar, M.R. Rahman, K.U. Bhat, *J. Mater. Sci.-Mater. Electron.* **32**, 20351 (2021)
8. Y. Guo, Z. Chen, W. Yang, K. Li, D. Yang, Q. Zhang, H. Wang, *ACS Appl. Mater. Interfaces* **13**, 55481 (2021)

9. S. Zhang, J. Xu, J. Yu, L. Song, J. He, N. Ma, X. Hou, X. Chou, *Mater. Lett.* **287**, 129271 (2021)
10. Y. Guo, Y. Cao, Z. Chen, R. Li, W. Gong, W. Yang, Q. Zhang, H. Wang, *Nano Energy* **70**, 104517 (2020)
11. Q. Zhang, Z. Zhang, Q. Liang, F. Gao, F. Yi, M. Ma, Q. Liao, Z. Kang, Y. Zhang, *Nano Energy* **55**, 151 (2019)
12. Z. Chen, Y. Cao, W. Yang, L. An, H. Fan, Y. Guo, *J. Mater. Chem. A* (2022). <https://doi.org/10.1039/D1TA08605G>
13. B. Li, H. Liu, Y. Sun, Z. Chen, Y. Zhang, Y. Guo, *Mater. Lett.* **310**, 131505 (2022)
14. P. Manchi, S.A. Graham, B. Dudem, H. Patnam, J.S. Yu, *Compos. Sci. Technol.* **201**, 108540 (2021)
15. Y. Guo, Z. Chen, H. Wang, Q. Zhang, *J. Inorg. Mater.* **36**, 919 (2021)
16. J.H. Zhang, X. Hao, *Nano Energy* **76**, 105074 (2020)
17. S. Gupta, R. Bhunia, B. Fatma, D. Maurya, D. Singh, Prateek, R. Gupta, S. Priya, R.K. Gupta, A. Garg, *ACS Appl. Energy Mater.* **2**, 6364 (2019)
18. B. Dudem, L.K. Bharat, H. Patnam, A.R. Mule, J.S. Yu, *J. Mater. Chem. A* **6**, 16101 (2018)
19. W. Seung, H.J. Yoon, T.Y. Kim, H. Ryu, J. Kim, J.H. Lee, J.H. Lee, S. Kim, Y.K. Park, Y.J. Park, S.W. Kim, *Adv. Energy Mater.* **7**, 1600988 (2017)
20. X. Wu, H. Liu, J. Chen, *J. Mater. Res.* **36**, 1153 (2021)
21. W. Huang, H. Liu, *J. Mater. Sci.-Mater. Electron.* (2021). <https://doi.org/10.1007/s10854-021-07336-w>
22. L. Zhang, X. Pu, M. Chen, S. Bai, Y. Pu, *J. Eur. Ceram. Soc.* **38**, 2304 (2018)
23. A. Xie, H. Qi, R. Zuo, *ACS Appl. Mater. Interfaces* **12**, 19467 (2020)
24. F. Pang, X. Chen, C. Sun, J. Shi, X. Li, H. Chen, X. Dong, H. Zhou, *ACS Sustain. Chem. Eng.* **8**, 14985 (2020)
25. J. Huang, H. Qi, Y. Gao, A. Xie, Y. Zhang, Y. Li, S. Wang, R. Zuo, *Chem. Eng. J.* **398**, 125639 (2020)
26. H. Qi, R. Zuo, *J. Mater. Chem. A* **7**, 3971 (2019)

Publisher's Note Springer Nature remains neutral with regard to jurisdictional claims in published maps and institutional affiliations.